Journal homepage: <http://www.ijaas.in>

## Enhancing Brain Tumor Detection with Xception and Grad-CAM: A Transfer Learning-Based MRI Analysis

Neeru Saxena <sup>1\*</sup>, Dr. Ajeet Singh <sup>2</sup><sup>1</sup> *Research Scholar, School of computing Science and Engineering, Galgotias University, India*<sup>2</sup> *Associate Professor, School of computing Science and Engineering, Galgotias University, India*

### ARTICLE INFO

### ABSTRACT

#### Article history:

Received: 21-05-2025

Received in revised form:

01-06-2025

Accepted: 13-07-2025

#### Keywords:

*Xception, Explainable AI (XAI), Segmentation, MRI, MobileOne S2*

The central organ of the human nervous system consists of brain that sends and receive stimuli to the different organs of the body in the engagement of daily routine activities. Irregular growth of the cells near the brain that disturb the normal function of the healthy brain cells that result in brain tumor. Timely diagnosis of a brain tumor is essential for effective treatment, improved results, and minimizing complications. Machine learning techniques are reliable for brain tumor detection that enables accurate analysis of medical data for identification of tumors with early and improve diagnostic efficiency. Transfer learning which is a machine learning algorithms can be able to achieve high accuracy with minimal training data by leveraging pre-trained models which can be able to adapt new tasks efficiently. Our study aims in brain tumor segmentation using MRI through Xception model which is a deep convolutional neural network. The aim of using xception model for its efficiency and strong feature extraction capabilities. Pre processed MRI images are given to caption based segmentation framework that recognizes tumor regions with high accuracy. Explainable AI (XAI) techniques such as Grad-CAM is integrated to enhance transparency and trust that highlights the critical regions influencing the model's prediction. This approach also ensures that model focuses on relevant regions rather than irrelevant surroundings. Xception attained the high accuracy of 97.35% whereas MobileOne S2 had given the strongest training performance indicating healthy learning capabilities. The combination of AI and image processing in MRI based tumor segmentation improves diagnostic accuracy that enables early detection and personalized treatment with speedy more reliable results than manual methods.

© 2025 The Authors. Published by IASE. This is an open access article under the CC BY-NC-ND license (<http://creativecommons.org/licenses/by-nc-nd/4.0/>).

### Introduction

Cancer is now-a-days major global health concern, evolving as one of the major causes of death amongst all age groups. One in every six deaths globally is due to cancer grading as this is the second leading source of death after cardiovascular diseases [1]. Incorrect diagnosis of brain tumor obstructs effective medical treatment and diminishes the chances of survival of patients. A common method for distinguishing brain tumors includes

examining the brain MRI images of the patients [2]. This technique becomes more time consuming and prone to human errors while dealing with varied data and various specific types of brain tumor. Computer-aided diagnosis (CAD) systems have meaningfully supported neuro-oncologists by assisting in tumor detection, classification, grading and the broadly researched classification of brain tumors into benign and malignant types [3]. These CAD systems employ magnetic resonance

imaging (MRI) of the brain, as MRI suggest superior soft tissue contrast compared to computed tomography (CT) images. Brain tumors are categorized as primary or secondary based on their origin with primary tumors, which initiate in the brain consisting for about 70% of all cases[4]. Secondary tumors that arise in other parts of the body and scatter to the brain account for the remaining 30% the greater part of which are malignant. These

types of tumors are extremely aggressive and lethal which is a challenging task to detect them. These types of tumors spread over other areas of the spinal cord and brain as well [5]. Traditional methods for brain tumor classification and detection through MRI trust on various feature extraction and classification algorithms with the challenge lying in finding the optimal combination of features and classifier.

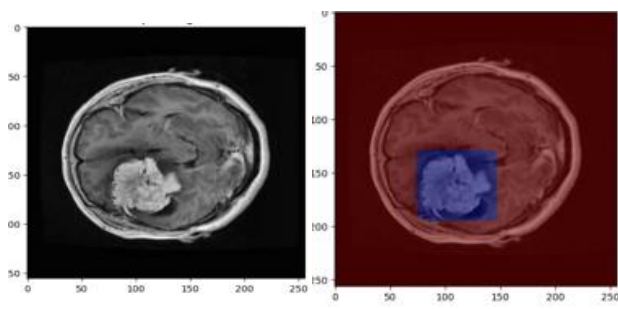


**Fig 1 Brain with tumor**

**Fig 2 Tumor with masking**

Programs analyses images by applying filters and mathematical techniques to arrays of pixels where each pixel signifies a specific color on the basis of systems like RGB, CMYK, or Gray scale. Pixels are interconnected creating relationships with adjoining pixels to jointly define features like edges, shapes, or specific objects[6]. The model uses mathematical equations and filters to recognize patterns in the pixels and extracts their properties as weighted values. Segmentation was done through faster R-CNN with the ResNet50 and classification of the tumor region was done through Alex Net transfer learning Model [7]. Three basic steps are followed for automatic classification and detection of brain tumor MRI. The noise of the image was cleaned through filter method in first stage. Each image's mean color moment was obtained through feature

extraction in the second stage. Classification of feature set that contain the color moment was done in the third stage [8]. Pre-trained deep learning models eliminate the requirement for large datasets and save time and multi-scale features were extracted from various layers, varies from low-level textures and edges to high-level objects and contours. For enhancing the classification performance the combining features from multiple bottom layers of pre-trained models was done in medical images [9]. The model consist of three successive 2D convolutional layers, each using 2x2 kernels. For evaluation performance the division of dataset was done as 85% for the training set and 15% for the validation set to evaluate performance. The performance of the proposed system was assessed using metrics such as precision,

accuracy, F1- score, sensitivity, specificity, and negative predictive value (NPV) [10]. Ten-fold cross-validation was done and the average results confirmed the efficiency of the proposed deep learning architecture (DLA) [11].

In this study, the comparison was done among six deep learning models for the segmentation of brain tumor in multi-contrast MRI scans. In our study the use of exception model for efficient extraction and accurate identification of tumor area in MRI images. XAI like Grad-CAM are applied which highlighted the important areas influencing predictions. This integration ensure reliable and interpretable results that increases trust and supporting clinical decision making process.

The remaining part of the paper is organized as follows: Section II summarize Literature Review, Section III outlines the proposed Methods, Section IV presents the results and outcomes, and Section V Conclusion.

## Literature review

### Literature Survey:

The performance comparison of AlexNet, GoogleNet and ResNet-18 pre-trained deep learning model was done and AlexNet model had achieved the highest accuracy of 99% [12]. The author presented three CNN models for highly accurate brain tumor classification. The first model perceives brain tumors with an accuracy of 99.33%, while the second model classifies tumors into five types with 92.66% accuracy. The third model classifies tumors into three grades, achieving 98.14% accuracy. The research

was first to fine-tune nearly all hyper parameters using grid search optimization [13]. The study of the researchers evaluated the performance of pre-trained ResNet50, VGG-16 and Inception v3 models in classification of 253 brain MRI images. VGG-16 achieved the highest accuracy at 94.42%, followed by ResNet50 with 82.49%. The findings was that transfer learning enhanced model performance when working with limited data. The comparison with other models the VGG-16 model demonstrated superior accuracy, showcasing the prospective of deep learning in automating brain tumor detection from MRI images [14]. This study evaluated a custom U-Net architecture using the TCGA-LGG dataset which had achieved pixel accuracies of 0.994 and 0.9975. The proposed model integrated dense-convolutional blocks, VGG16 pre trained layers, and Batch Normalization to improve performance [15]. The researchers had proposed two deep learning models for both binary classification and multiclass classification brain tumor. The researchers had applied 23 layers convolutional neural network (CNN) on first dataset as there was a large number of MRI scans for training purpose. When the same 23 layer CNN was applied on limited dataset, the over fitting problem was faced. To resolve this issue integration of transfer learning with VGG16 architecture was done. Upon comparison the model had achieved the accuracy upto 97.8% and 100% classification accuracy [16]. The study proposed classification system that adopted the concept of deep transfer learning and Google Net pre trained model was used for extracting feature from brain MRI scans. The experiment employed a patient-level five-fold cross-validation process on an MRI

dataset and 98% mean classification accuracy was attained [17]. The study introduced a new fully automatic algorithm that segments the entire cerebral venous system in MRI scans by utilizing morphological, structural, and relaxometry features. ELM which was a type of learning algorithm consisting hidden nodes of one or more layers was applied. A probabilistic neural network classification system was used to train and evaluate the accuracy of tumor detection in images, achieving an accuracy rate of 98.51%. [18]. The study had applied Weiner filter with various wavelet bands to de-noise and improve the input slices. The tumor pixel's subsets of were found with Potential Field (PF) clustering. Global threshold and various mathematical morphological operations were used to separate the tumor region in Fluid Attenuated Inversion Recovery (Flair) and T2 MRI. Local-Binary-Pattern(LBP) was fused with Gabor-Wavelet-Transform (GWT) features were used for accurate classification [19]. To improve classification accuracy and handle huge amount of data the researchers had proposed deep learning-based classification model containing five key modules. Skull stripping and pre-processing were done by using a guided bilateral filter (GBF). Next segmentation was done on tumor regions with the help of thresholding technique. Essential

texture and edge features were extracted through improved Gabor wavelet transform (IGWT). For refining the feature set the black widow adaptive red deer optimization (BWARD) algorithm were used for selecting the most relevant features. In the last classification is carried out using a hybrid Elman bidirectional long short-term memory (EBiLSTM) network [20]. The authors had proposed integrating a Convolutional Neural Network (CNN) with a Long Short-Term Memory (LSTM) network, leveraging LSTM's ability to improve feature extraction in CNNs. The hierarchical LSTM-CNN architecture demonstrated greater performance in classification of image tasks compared to traditional CNN-based methods [21]. The authors had proposed an automatic technique for detecting brain tumor using MRI scans was a multistep process. Initially brain MRI images undergo pre-processing to improve visual quality. Next two pre trained deep learning models were engaged to remove robust structures which are then compounded into a hybrid feature vector using the partial least squares (PLS) method. Afterwards, agglomerative clustering was utilized to find the most significant tumor areas. Finally, these detected regions are resized to a standard dimension and progressed to the head network for classification [22].

**Table 1: Comparative Analysis of proposed model with classification accuracy**

Year	Proposed Model	Dataset	Measurement
2022 [23]	CNN architecture focussing on Res Net, Alex Net and VGG. CNN and Data augmentation	Kaggle Dataset with 253 MRI images	Shown high detection accuracy and good evaluation value even with restricted dataset
2022 [24]	23 layers CNN with Transfer Learning VGG16 with 23	Two Publicly available dataset with 3064 and 152 MRI	Model's performance was improved by using the strength of

	Layers CNN	images	both architectures.
2022 [25]	CNN with transfer learning concept which reduced the large amount of data and minimizes the training and computation time		The accuracy of ResNet is better in comparison with VGG16 and InceptionV3
2022 [26]	Automated diagnosis process and use of ResNet50, EfficientNetB1, Efficient Net V2B1 Efficient Net Pre trained Convolutional Neural Networks (CNN) for the classification of brain tumor. Classification of 3 types of tumors with one class of non tumors	Fig share, SARTAJ and Br35H dataset with total 7022 MRI images.	87.67% and 89.55% training and validation accuracy with EfficientNetB1
2023 [27]	CNN Model for Brain Tumor classification capability of good generalization with good execution speed	3064 T1 Weighted contrast enhanced MRI from two hospitals	Classification accuracy 98.04%. Recall, precision and f1 score success rate 98%.
2023 [28]	Classification was done for two classes: Gloima and Pitutary tumors. Single-Image-Super-Resolution (SISR) used to enhance the MRI image for improving their fundamental features that helps in model training. Performance evaluation done by receiver operating characteristics curve (ROCC), error matrix, precision and recall.	1800 MRI images	VGG19 testing accuracy 99.98% and ResNext101_32 with testing accuracy 100%.
2024 [29]	Low order model like Proper Orthogonal	Brat 2018 dataset with 680 images.	Accuracy 95.88% with 1/3 <sup>rd</sup> of

	Decomposition (POD) and explainable AI like SHAP coupled with Convolutional Neural Network (CNN) for investigating 2D MRI scan. The POD-CNN output compared among Pre-trained models like MobileNetV2, Inception-V3, ResNet101, VGG-19		computational time.
2024 [30]	Multi-scale Fractal Feature Network (MFFN) used for segmentation of brain tumor leveraging fractal residual deep learning and a multi-scale approach. Detection accuracy improved with the help of MFFN by preserving tumor integrity and enhancing sensitivity by reducing redundant tumor region.		94.66% accuracy, 94.42% sensitivity, 92.81% specificity using five fold cross validation.
2024[31]	The Convolutional Stacked Auto encoder Network (C-SAN) was developed to detect brain tumors using MRI images. The process starts with Non-Local Means (NLM) for pre-processing followed by V-Net-based Segmentation. Feature extraction done through Grey Level difference statistics. C-SAN along with CNN and Deep stacked Auto encoder (DSAE)	Brats 2018 and Fig share dataset	Accuracy 90.9%, sensitivity 95.8%, specificity 92.8%

	employed for accurate brain tumor detection.		
--	--	--	--

**Challenges:**

- High-quality, labeled MRI datasets are rare, making it tough to train deep learning models efficiently and avoid over fitting.
- Large models incline to over fit when trained on small datasets, necessitating transfer learning or data augmentation strategies to simplify well.
- Deep learning models particularly CNNs and hybrid architectures need substantial computational resources making real-time processing challenging.
- MRI images often contain noise, motion artifacts, and intensity variations which affect model performance and necessitating advanced pre-processing methods.
- Variability in MRI attainment protocols, scanner types and imaging conditions affects model simplification across diverse datasets.
- Tumors have irregular shapes, unclear boundaries and varying intensities making pixel-wise segmentation difficult even with advanced techniques like U-Net.

**MATERIALS AND METHODS**

This section deals with resources and procedures used in this research. The materials comprises of data sources, hyper parameters, environments and metrics. The

methods tells about the procedures used in creating a transfer learning model capable of detecting brain tumors.

**Materials**

The dataset which is used in our study is divided into three categories: the validation set, testing set and training set. The total dataset size is 2146 images 321 test images. The purpose of validation set is to check the accuracy of the model which has been trained using the training set and if the accuracy is still supposed to be not qualified then right hyper parameter will be searched. Then training of the model is again carried out. This state is done to prevent over fitting which could occur if the model were assessed using only the testing set. The training set helps the model study to detect brain tumors, while the testing set is used to measure its performance and test the created prototypes. The data splitting ratio was kept 20% for the validation and 80% for training set performed on Kaggle Br35H dataset. Training and validation images are fed into a GradCAM model built on the Xception backbone. The trained network is tested with the testing images that was selected randomly to locate the tumor. The local tumor masks are then merged with their corresponding original scans once more to get the tumor segments from the images.

## Difference between Manual segmentation and automated segmentation through MRI

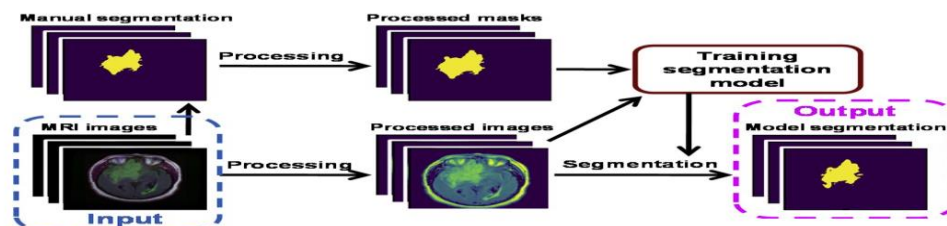


Fig 3 manual segmentation vs. automated segmentation

Manual segmentation of brain tumor detection through MRI involves a radiologist who accurately outlines the tumor boundaries on MRI scans slice by slice. This process is initiated with obtaining high resolution MRI images using sequences like T1-weighted, T2-weighted, FLAIR and contrast enhanced scans.. The review is done through expert by viewing each image to identify the tumor region based on intensity, shape and contrast with surrounding tissues. With the help of specialized software the manual tracing is done to find out tumor contours and ensuring accuracy in defining the tumor core, edema and necrotic areas. The segmentation process is performed across all relevant slices to reconstruct 3D tumor volume which is a time consuming process and require deep anatomical knowledge and clinical experience. Despite its exactness manual segmentation is subjective and varies among experts. It aids as a ground truth for validating automated segmentation model.

The automated segmentation of brain tumor detection through MRI influences machine learning and deep learning algorithms to identify and outline the tumor region with minimal human interference. Convolutional Neural Network (CNN) is one of the technique which is use to analyse MRI scans and

classify the tissues into tumor and no tumor regions which is known as classification technique. The process is initiated with the pre processing steps such as normalizaion and skull stripping trailed by model implication to generate segmentation masks . Automated methods reduce time, enhance reproducibility and minimizes expert’s variability. These models are trained on specific datasets and validated against manual segmentation that support accurate diagnosis, planning for treatment and help in monitoring neuro-oncology.

### Algorithm for brain tumor segmentation using Pre-trained models

#### Inputs:

- Model used : CNN,mobileone\_s2,mobilenet\_v2, resnet50,efficientnet\_b0, densenet169 , xception for segmentation
- Dataloader for training dataset
- Dataloader for validation dataset
- Dataloader for testing dataset
- Loss function with BCEWithLogitsLoss
- Optimizer used : Adam
- Computation device: CPU

#### Step 1: Training the Model (train\_epoch (where no. of epochs = 10))

1. Set the model to training mode.
2. Initialize `total_loss`, `correct_pixel_count`, and `total_pixel_count`.
3. For each batch of images and masks in the training set:
  - Move data to the selected device.
  - Initialize optimizer gradients to zero.
  - Obtain prediction by performing forward pass.
  - Using predicted and true masks compute loss.
  - Backpropagate the loss.
  - Update the model through parameters with the optimizer.
  - To get binary prediction apply sigmoid activation and threshold the output at 0.5.
  - Update the total by calculating the number of correctly predicted pixels.
4. For each epoch compute and return average training loss and pixel-wise accuracy.

### **Step 2: Validating the Model (validate\_epoch)**

1. Set the model to evaluation mode.
2. Initialize `total_loss`, `correct_pixel_count`, and `total_pixel_count`.
3. For each batch (batch size=4) of images and masks in the validation set:
  - Move data to the device.
  - To obtain prediction perform a forward pass.
  - Without updating model parameters compute loss.
  - To get binary prediction apply sigmoid and threshold.
  - Calculate the number of correctly predicted pixels.
4. Calculate `average_validation_loss` and pixel-wise accuracy.

### **Step 3: Testing the Model (test\_model)**

1. Set the model to evaluation mode.
2. Initialize `total_loss`, `correct_pixel_count`, and `total_pixel_count`.
3. Masks in the test set for each batch of images :
  - Move data to the device.
  - To get prediction perform a forward pass.
  - Loss will be computed.
  - To get binary prediction apply sigmoid and threshold.
  - The number of correctly predicted pixels will be Counted.
4. Average test loss and pixel-wise accuracy will be computed and return.

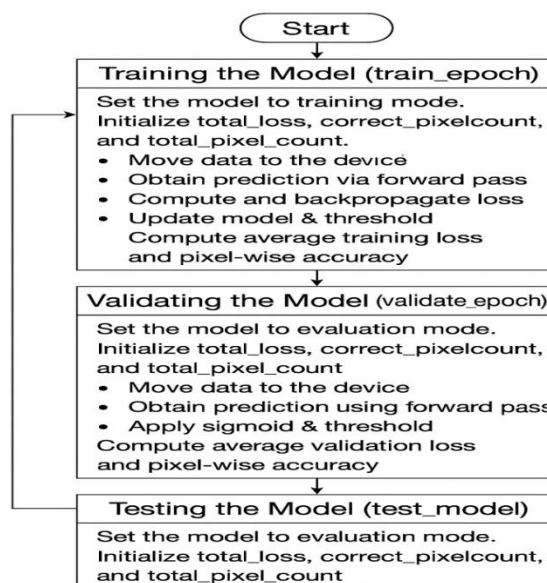


**Fig 4 Deep Learning Model Lifecycle: Training, Validation, and Testing Pipeline**

**Pre Processing** The pre processing was initiated with loading of multi modal MRI scans T1, T2 FLAIR and T1 contrast sequences. These images first converted using gray scale converter of size  $256 \times 256$ . As such there was no noise in the images so none of the noise removal technique was used. These images were aligned using registration techniques for ensuring spatial consistency. Skull stripping technique was used for removing non brain tissues trailed by intensity normalization for standardizing the pixel values across MRI scans. Resizing and cropping were applied so that the dimension of input image should be as per xception model requirement that is  $256 \times 256$ . The model requirement is that all images should be of fixed size. Data augmentation technique such as flipping, rotation and contrast adjustment was applied to increase dataset variability and enhance model generalization. Finally ground truth masks are binarized and associated with their corresponding

images. This pre-processed data is then given to xception model which uses depth wise separable convolutions for efficiently extracting spatial and related features for accurate tumor segmentation.

**Model preparation** Model preparation for brain tumor segmentation using MRI through Xception model involves altering the original architecture which was designed for classification into a segmentation network. The fully connected layer was removed and substituted with a decoder or up sampling path frequently followed U-Net style design. The altered model took pre processed MRI slices as input and pixel wise probability map as an output with the help of sigmoid activation. Transposed convolutions was added to recover spatial details lost during down sampling. This revision allowed the xception model to achieve accurate semantic segmentation of brain tumors from MRI images.

**Training** The training process for brain tumor segmentation using xception model initiated by using Binary Cross entropy

Logits as the loss function that is suitable for binary classification job such as classifying two class tumor and non tumor with the help of pixel prediction. Adam optimizer was used to optimized which is known for its adaptability and efficiency in deep learning application. Pre processes MRI scans along with their ground truth segmentation masks were served into the model in mini batches sizes of 4 for efficiently utilizing computational resources and stabilized the training process. Each input batch pass through the forward pass through the model for producing segmentation prediction, which were then compared to the ground truth to computer. The loss was back propagated to update the model weights. Training was conducted in multiple epochs which is 10 epochs which allow the model to gradually learn and refine its prediction. During the entire training process, key metrics such as loss and pixel wise accuracy were monitored for assessing learning progress and detect over fitting.

**Validation** During the validation phase the evaluation of the xception model was done on separate set of unseen MRI data which was not used during training. This step is necessary for assessing the model's ability

to generalize the new inputs. The model was set to evaluation by disabling the gradient computation and guaranteed consistent behavior. Each MRI image in the validation set was passed through the model to generate predicted segmentation mask which was then compared to the ground truth mask. Pixel wise accuracy, Dice coefficient and intersection over union (IoU) were calculated for evaluating the segmentation quality.

**Testing** In testing phase the firnal trained xception model was applied on a separate test dataset for evaluating its real world performance. The model processed each test MRI image to generated segmentation mask for predicting the area likely to contain brain tumors. These predicted masks were then compared with the ground truth observations to assess the model's effectiveness. Pixel wise accuracy, Dice coefficient and IoU were computed to calculate model's performance. This step provided and unbiased evaluation and confirm whether the model generalizes well and can consistently segment brain tumor on previously unseen MRI images in practical scenarios.

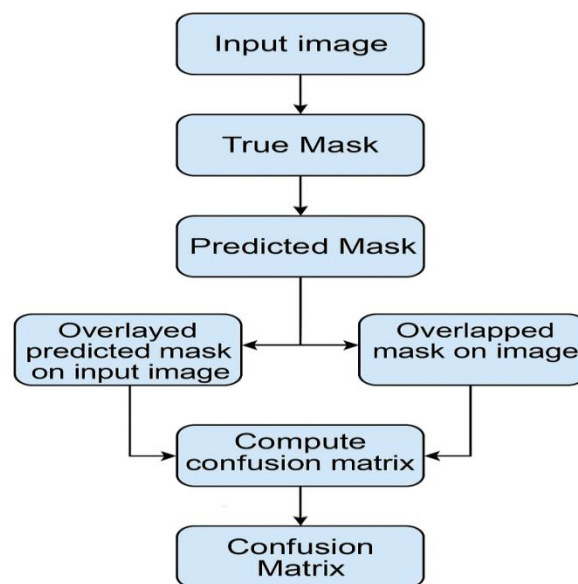


**Fig 5 Segmentation Workflow and Evaluation Pipeline**

$X \in \mathbb{R}^{H \times W}$  be the input MRI image (grayscale, with height  $H$  and width  $W$ )

$f_\theta(X)$  be the deep learning model with parameters  $\theta$

$Y = f_\theta(X)$  be the predicted segmentation mask

$Y_{\text{pred}} = f_\theta(X)$ : predicted segmentation by the model

$Y_{\text{true}} \in \{0,1\}^{H \times W}$ : **true mask** (ground truth annotation by a radiologist)

$Y_{\text{pred}} = f_\theta(X) \in \{0,1\}^{H \times W}$ : **Predicted mask** (model's output indicating tumor region)

$L(Y_{\text{pred}}, Y_{\text{true}})$ : loss function measuring difference between prediction and true mask

$S(X)$  be the saliency or attention map generated by XAI methods (e.g., Grad-CAM)

**Input Image:** Input image means providing the raw data to the model consisting of MRI scans. In context to Explainable AI (XAI) which features within the image influences the model's

prediction. The accuracy and reliability of the segmentation depends upon the model interpretation is the right part of the image. The main goal of XAI is to ensure that the emphasizes on medically relevant areas such as tumors rather than distracted by irrelevant background structure or artifacts.

$$Y = f_\theta(X), \text{ where } S(X) = \partial X \partial f_\theta(X) \quad (1)$$

**True Mask:** The true mask means the representation of the ground truth annotation which is provided by the radiologist who highlights the tumors which is our area of interest in the medical images. The mask served as benchmark against which is the model's predictions are evaluated to measure accuracy and reliability. XAI compares the model's predicted output with the expert generated true mask which is essential. If model's segmentation closely matches with human explanation which indicates that the model has learned meaningful and relevant features. This alignment increases trust in the decision making process made by the

model and supports its practical deployment.

$$Y_{true}(i,j) = \begin{cases} 1 & \text{if pixel (i,j) belongs to tumor region} \\ 0 & \text{otherwise} \end{cases} \quad (2)$$

In context with XAI

$$\left\{ \begin{array}{l} \text{Support} \\ \text{Support} \end{array} \right. (S(X)) \approx \text{Support}(Y_{true}) \quad (3)$$

**Predicted mask:** The predicted mask means the model's output by highlighting the region it recognizing as corresponding to tumor which is our object of interest. XAI verify whether predicted mask aligns with recognized domain knowledge domain knowledge and expert explanation. If the predicted deviates from expectation then further investigation is essential to find out the reason behind it. GRAD CAM can be use to visualizes and interpret the model's focus area that enhances transparency and trust.

$$Y_{pred}(i,j) = \begin{cases} 1 & \text{if pixel (i,j) is predicted as tumor} \\ 0 & \text{otherwise} \end{cases} \quad (4)$$

The alignment condition for trust and interpretability is:

$$\text{Support}(Y_{pred}) \approx \text{Support}(G(X)) \approx \text{Support}(Y_{true}) \quad (5)$$

If there is a large deviation:

$$|\text{Support}(Y_{pred}) - \text{Support}(Y_{true})| \gg 0 \quad (6)$$

**Over layed Predicted Mask on Input Image :** Overlaying the predicted mask on the original input image that highlights

where the model is focusing. This technique gives the clear way to understand the regions identified by the model as important. XAI visualizes which are extremely valuable for the non-technical users like doctors .They permits experts to speedily and easily verify whether the model is correctly identifying medically relevant tumor region. This visual confirmation builds faith in the model's output support its adoption in decision making process.

Let

$Y_{pred} \in \{0,1\}^{H \times W}$ : Predicted binary mask (1 = tumor region, 0 = background)

$\alpha \in [0,1]$ : Transparency factor for overlaying

V: Visualized image with overlay

Then, the **overlay image** VVV can be represented as:

$$V(i,j) = (1-\alpha) \cdot X(i,j) + \alpha \cdot C \cdot Y_{pred}(i,j) \quad (7)$$

C is a constant or color map applied to the tumor region (e.g., red color for tumor)

V(i,j) blends the gray scale intensity with the highlighted region

**Overlapped Mask on Image:** The overlapped mask visualization includes filling the predicted mask directly on the original image that provides more distinct and clear boundaries of the detected region. This technique increases the visibility of the segmented region making it to easier to evaluate the model's performance. XAI is beneficial as it simplifies the comparisons between predicted region and the actual ground truth annotation. With the help of

highlighting it becomes easier to identifying the under segmentation and over segmentation instances that allows the users to pinpoint where model is missing the important details or incorrectly labeling extra areas.

Let

$\alpha, \beta \in [0,1]$ : Transparency factors for overlaying

$C_p, C_t$ : Color encodings for predicted and true masks respectively

$V$ : Final visualization image

Then, the overlap visualization can be represented as:

$$V(i,j) = (1-\alpha-\beta) \cdot X(i,j) + \alpha \cdot C_p \cdot Y_{pred}(i,j) + \beta \cdot C_t \cdot Y_{true}(i,j) \quad (8)$$

**Compute Confusion Matrix :** The computation of confusion matrix includes a detailed pixel by pixel comparison between the true mask and predicted mask which results in evaluation metrics such as True Positive (TP), False Positive (FP), True Negative (TN), False Negative (FN) that collectively describes the model's performance. In context of XAI these metrics provide transparency into how accurately and reliably the model is functioning. By knowing the strength and weaknesses users and experts can understand the areas of success as well as potential errors. High FP indicates that model is being overly sensitive as well as high FN indicates that there are points to missed detection.

$$TP = \sum_{i,j} 1 [Y_{true}(i,j) = 1 \wedge Y_{pred}(i,j) = 1]$$

$$TN = \sum_{i,j} 1 [Y_{true}(i,j) = 0 \wedge Y_{pred}(i,j) = 0]$$

$$FP = \sum_{i,j} 1 [Y_{true}(i,j) = 0 \wedge Y_{pred}(i,j) = 1]$$

$$FN = \sum_{i,j} 1 [Y_{true}(i,j) = 1 \wedge Y_{pred}(i,j) = 0]$$

$1[\cdot]$  is the indicator function that returns 1 if the condition is true, otherwise 0

**Confusion Matrix:** The final step includes displaying the confusion matrix as a heatmap that provides a clear and visual representation of model's performance. Heatmaps allows stakeholders to easily quantify the outcome of the model's prediction. Each cell visually transmits the number of true positive, false positive, true negative and false negatives making the evaluation straightforward and available. XAI translate the raw model performance into interpretable number which increases transparency and enhances trust.

## RESULTS AND OUTCOMES

The objective of this study is to measure the performance of various pre trained deep learning models for brain tumor segmentation using MRI. Although to calculate accurate segmentation is very difficult for diagnosis, treatment planning and brain tumors monitoring. The comparison of U-Net architecture with various pre trained models such as CNN, mobileone\_s2, mobilenet\_v2, resnet50, efficientnet\_b0, densenet169, xception. The models are assessed through key metrics like Dice score, Intersection over Union (IoU), Precision, and Recall. By identifying the effectiveness of models our study aims at improving automated tumor detection accuracy and provide the support to the clinical experts in decision making.

**Dataset:** The dataset used were Br35H with 2146 total images and 321 test images. The use of a large dataset permits for extensive training, validation, and testing, enabling an in-depth evaluation of

Br35H's performance across numerous conditions. The results of this study support the development of deep learning methods and offer meaningful insights for future enhancements in image recognition technologies.

Table 4.1 compares the performance of numerous deep learning models for an image segmentation task and show the matrices of accuracy scores for training, validation and testing sets.

**Table 2: Comparative analysis of various Pre trained model and accuracy**

S.No.	Model Name	Training Accuracy (%)	Validation accuracy (%)	Testing accuracy (%)
1	resnet50	98.9618	97.3438	97.3438
2	efficientnet-b0	98.8121	97.2115	97.2115
3	mobilenet_v2	98.603	97.056	97.056
4	mobileone_s2	99.0321	97.2982	97.2982
5	densenet169	98.9762	97.0555	97.0555
6	Xception	99.3025	97.3522	97.3522

The table exhibits the training, validation, and testing accuracy of six different deep learning models evaluated for a segmentation task. Among the models, **Xception** attained the highest testing accuracy at **97.35%**, indicating superior generalization abilities, followed closely by **ResNet50** and **MobileOne\_S2**. **MobileOne\_S2** recorded the highest training accuracy at **99.03%**, suggesting strong learning capacity though its slightly lower validation accuracy suggestions at slight over fitting. **EfficientNet-B0** and **DenseNet169** delivered balanced performance with training accuracies

above **98.8%**, and validation and testing scores around **97.05%**, showing consistent learning but slightly less precision than the top performers. **MobileNet\_v2**, while slightly behind maintained competitive accuracy and possible offers benefits in model efficiency and speed. Overall, all models demonstrate high effectiveness with testing accuracies exceeding **97%**, showcasing their suitability for the task.

However, adjustments between model complexity, training time, and marginal accuracy gains should guide the selection for deployment in real-world scenarios.

**Table 3: Training configuration and hyper parameters**

Training Parameters	Value
Total size	2146
Training size	1824
Test Size	322
No. of epochs	10
Learning Rate	0.0001
Batch size	4
Optimizer	Adam
Image Shape	256,256

(Grayscale)
-------------

The table summarizes the key training parameters and hyper parameters used in the deep learning model development process. A total of **2,146 gray scale images** with a resolution of **256×256 pixels** were used out of which **1,824** were used for training and **322** for testing. The model was trained over **10 epochs**, which balances computational efficiency with adequate learning opportunities. A **batch size of 4** was selected allowing for recurrent weight updates and making the model appropriate for systems with limited

memory. The **Adam optimizer** was employed due to its adaptive learning rate and efficiency in handling sparse gradients. A **learning rate of 0.0001** was chosen to guarantee gradual and steady convergence minimizing the risk of missing the optimal point. The grayscale format minimizes computational complexity while retaining essential image features. These settings imitate a well-balanced method aimed at attaining high accuracy while maintaining computational effectiveness and avoiding over fitting.

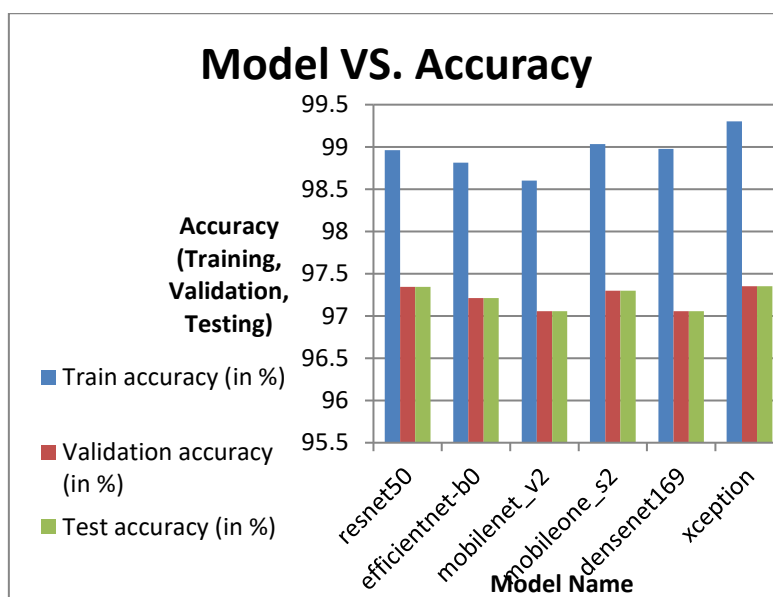


**Fig 6 Comparison of various models with accuracy**

The performance comparison of six deep learning models – ResNet50, EfficientNet-B0, Mobile Net V2, Mobile One S2, DenseNet169 and X ception based on training, validation and testing accuracies. Accuracy percentages ranging from 95.5% to 99.5% are on vertical axis whereas horizontal axis consists of model names. Each model has three bars blue for

training, red for validation and green for test accuracies.

Although all models establish high training accuracy with X ception model attaining the highest accuracy at approximately 99.3%. MobileOneS2 and ResNet50 also achieve well with training accuracy approximately 99%. Only training accuracy alone is not sufficient, validation

and test accuracies also indicate how well a model simplifies on unseen data. Mobile One S2 and Xception exhibits strong generalization with validation and test accuracies of 97.3%. Mobile Net V2 shows the lowest validation and test performance of 97% despite high accuracy on training signifying possible over fitting.

The difference between training and validation or test accuracies in some model

like ResNet50 and Xception signify the risk of over fitting. Overall Xception and Mobile One S2 exhibit a good balance between learning and generalization opting them a strong candidate for healthy model performance across datasets. This graph aids in identifying that model that are not only accurate but also reliable.



Fig 7 Comparison of various model with training loss

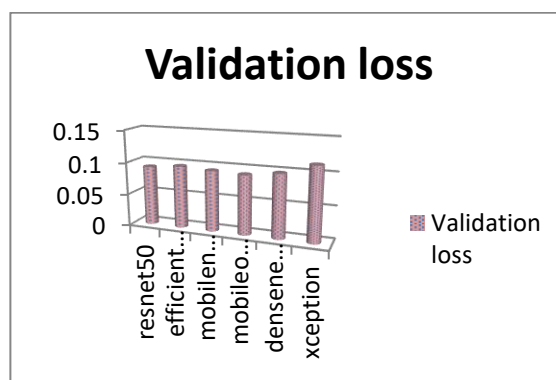


Fig 8 Comparison of various model with validation loss

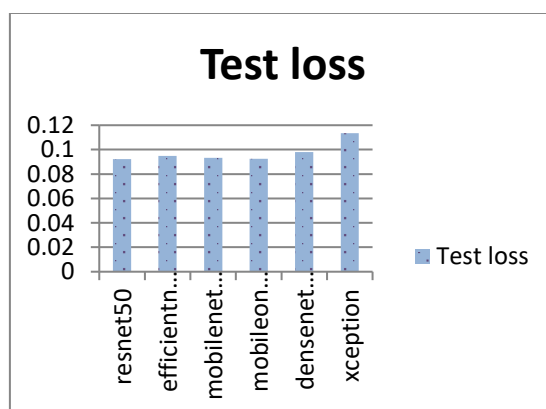


Fig 9 Comparison of various model with test loss

The above three graphs demonstrate the train, validation, and test losses of numerous deep learning models i.e. ResNet50, Efficient Net, Mobile Net,

Mobile One, Dense Net, and Xception which are used for brain tumor segmentation. Xception attained the lowest train loss which is the indication of strong

learning on training data followed closely by Dense Net and Mobile One. In validation loss all models had given the similar results with Xception and Dense Net slightly outperforming as compared to others showing good generalization during training. Xception showed the highest test

loss which means that potential over fitting and limited generalization to unseen data. On the contrary ResNet50 and Efficient Net verified lower test losses which is the indication of more reliable performance and better generalization in real-world testing scenarios.

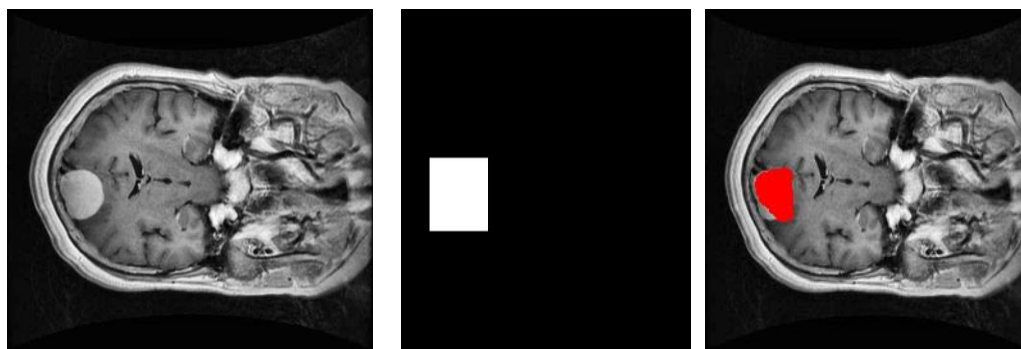


**Fig 10(a) Original image   Fig 10 (b) Target mask image   Fig 10(c) Predicted Mask overlap on image**

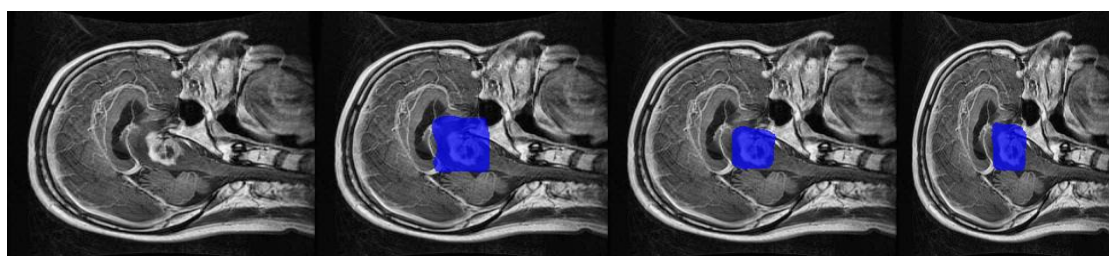
The above three images represents a brain segmentation process using MRI scans. Figure 7 which is the original image is a grayscale axial MRI scan of human brain. This image exhibits a clear, round and well defined mass in the left frontal lobe region. The bright intensity and well circumference border advise a space occupying lesion can likely be tumor. This image can be the input for segmentation and diagnosis.

Figure 8 is a black and white image which is a binary segmentation mask that represent the region of interest (ROI) corresponding to the tumor area in the original MRI. The rest of the image is black that indicates the non-tumor region. Such binary masks are used in machine learning to train or validate the models in the tasks like tumor detection and localization.

Figure 9 shows the result of overlaying the segmented tumor from the binary mask on

the original MRI. The tumor are is highlighted in red exactly matching the location of the white mass seen in the first image. This visualization technique helps the medical experts about the confirmation of accuracy of automatic tumor detection and helps in planning for further diagnosis.

All these images illustrate the process of identifying and separating a brain tumor using MRI scans and segmentation techniques. The original image detects the irregularities, the binary mask marks the region of computational processing or region of interest and overlay visually authenticates the segmentation. This approach plays an important role in medical diagnostics where AI empowered tools increases the accuracy and speed of identifying brain abnormalities.



**Fig 11(a) Original image Fig11(b) DenseNet169 Fig 11(c) EfficientNet-b0 Fig 11(d) MobileNet\_V2**

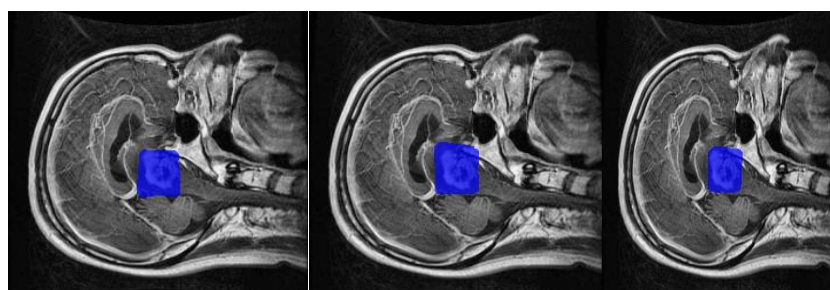


**Fig 11(e) Mobile one S2 Fig 11(f) ResNet50 Fig 11(g) Xception**

The images demonstrate the results of brain tumor segmentation on MRI scans with highlighted blue regions which is the indication of detected tumor areas. The first image exhibit the original MRI without segmentation. The succeeding images display the outputs from various segmentation models exhibiting varying precision in localizing the tumor. Some segmentations cover larger areas possibly including irrelevant regions while others more accurately isolate the tumor. The advanced segmentations suggest improved model performance. These visualizations support the use of **Explainable AI (XAI)** particularly Grad-CAM to verify that the model's focus aligns with the actual tumor, enhancing interpretability, trust, and diagnostic reliability. Based on the above images the model generating the most

accurately localized and compact tumor segmentation with minimal inclusion of surrounding tissue is the **Xception model** which is the indication of its superior performance.

## CONCLUSION

The combination of artificial intelligence (AI) and image processing techniques into the medical imaging field has transformed the diagnosis and monitoring of brain tumors. In this study series of images analyzed that demonstrates a clear and efficient workflow for brain tumor segmentation using MRI. The original MRI image helps in the foundation for identifying abnormal structures whereas the binary mask isolate the tumor area with high accuracy. The final overlay image serves as a visual confirmation of tumor's

location which increases the interpretability and clinical value of the automated process.

Such segmentation method play an essential role in enhancing diagnostic accuracy, enable early detection and help in providing personalized treatment planning. Manual tumor identification by radiologist is time consuming and subject to human variability. At the same time AI assisted segmentation offers reliable and speedy results minimizes workload and enhancing efficiency in clinical settings.

The use of marks binary masks and overlays supports the training of deep learning models that can simplify across large datasets and varied patient populations. These models continue to progress driven by advancements in computational power and access to marked medical datasets.

In conclusion the integration of MRI imaging and AI-based segmentation not only help in accurate tumor detection but also supports serious decision making in neurology and oncology. AS these technologies developed they promise to improve patient outcomes by enabling speedy and more exact intervention.

The future of brain tumor detection and segmentation using AI and medical imaging is very promising . AS deep learning models become more sophisticated the greater accuracy, robustness and generalization can be expected among varied patient demographics and imaging modalities. One more future scope is real time tumor detection combined directly with MRI scanners allow immediate feedback during imaging methods. This can assist

radiologist to take faster and informed decision during patient evaluation.

## Reference

- [1] S. A. Abdelaziz Ismael, A. Mohammed, and H. Hefny, "An enhanced deep learning approach for brain cancer MRI images classification using residual networks," *Artif. Intell. Med.*, vol. 102, p. 101779, 2020, doi: 10.1016/j.artmed.2019.101779.
- [2] P. Sharma and A. P. Shukla, *Brain Tumor Classification Using Convolution Neural Network*, vol. 341. Springer Singapore, 2022. doi: 10.1007/978-981-16-7118-0\_50.
- [3] S. Deepak and P. M. Ameer, "Brain tumor classification using deep CNN features via transfer learning," *Comput. Biol. Med.*, vol. 111, no. June, p. 103345, 2019, doi: 10.1016/j.compbiomed.2019.103345.
- [4] P. Nagaraj, V. Muneeswaran, L. Veera Reddy, P. Upendra, and M. Vishnu Vardhan Reddy, "Programmed Multi-Classification of Brain Tumor Images Using Deep Neural Network," *Proc. Int. Conf. Intell. Comput. Control Syst. ICICCS 2020*, pp. 865–870, 2020, doi: 10.1109/ICICCS48265.2020.9121016.
- [5] N. Noreen, S. Palaniappan, A. Qayyum, M. Imran, and M. Shoaib, "A Deep Learning Model Based on Concatenation Approach for the Diagnosis of Brain Tumor," *IEEE Access*, vol. 8, pp. 55135–55144, 2020, doi: 10.1109/ACCESS.2020.2978629.
- [6] C. L. Choudhury, "Brain Tumor Detection and Classification Using Convolutional Neural Network and

- Deep Neural Network,” pp. 0–3.
- [7] V. Rajinikanth, A. Noel, J. Raj, K. P. Thanaraj, and G. R. Naik, “applied sciences A Customized VGG19 Network with Concatenation of Deep and Handcrafted Features for Brain Tumor Detection”.
- [8] A. Diker, “A performance comparison of pre-trained deep learning models to classify brain tumor,” *EUROCON 2021 - 19th IEEE Int. Conf. Smart Technol. Proc.*, no. July, pp. 246–249, 2021, doi: 10.1109/EUROCON52738.2021.9535636.
- [9] H. A. Khan, W. Jue, M. Mushtaq, and M. U. Mushtaq, “Brain tumor classification in MRI image using convolutional neural network,” *Math. Biosci. Eng.*, vol. 17, no. 5, pp. 6203–6216, 2020, doi: 10.3934/MBE.2020328.
- [10] G. Cabanac, C. Labbé, and A. Magazinov, “Tortured phrases: A dubious writing style emerging in science. Evidence of critical issues affecting established journals,” 2021, [Online]. Available: <http://arxiv.org/abs/2107.06751>
- [11] J. Amin, M. Sharif, A. Haldorai, M. Yasmin, and R. S. Nayak, “Brain tumor detection and classification using machine learning: a comprehensive survey,” *Complex Intell. Syst.*, vol. 8, no. 4, pp. 3161–3183, 2022, doi: 10.1007/s40747-021-00563-y.
- [12] R. Mohan *et al.*, “Journal of Population Therapeutics & Clinical Pharmacology,” vol. 28, no. January, 2022, doi: 10.47750/jptcp.2022.873.
- [13] E. Irmak, “Multi-Classification of Brain Tumor MRI Images Using Deep Convolutional Neural Network with Fully Optimized Framework,” *Iran. J. Sci. Technol. - Trans. Electr. Eng.*, vol. 45, no. 3, pp. 1015–1036, 2021, doi: 10.1007/s40998-021-00426-9.
- [14] O. Sevli, “Performance Comparison of Different Pre-Trained Deep Learning Models in Classifying Brain MRI Images,” *Acta Infologica*, vol. 5, no. 1, pp. 141–154, 2021, doi: 10.26650/acin.880918.
- [15] S. Ghosh, A. Chaki, and K. Santosh, “Improved U-Net architecture with VGG-16 for brain tumor segmentation,” *Phys. Eng. Sci. Med.*, vol. 44, no. 3, pp. 703–712, 2021, doi: 10.1007/s13246-021-01019-w.
- [16] M. S. I. Khan *et al.*, “Accurate brain tumor detection using deep convolutional neural network,” *Comput. Struct. Biotechnol. J.*, vol. 20, pp. 4733–4745, 2022, doi: 10.1016/j.csbj.2022.08.039.
- [17] S. Deepak and P. M. Ameer, “Brain tumor classification using deep CNN features via transfer learning,” *Comput. Biol. Med.*, vol. 111, p. 103345, 2019, doi: 10.1016/j.compbiomed.2019.103345.
- [18] Z. Jia and D. Chen, “Brain Tumor Identification and Classification of MRI images using deep learning techniques,” *IEEE Access*, vol. 1, pp. 1–1, 2020, doi: 10.1109/access.2020.3016319.
- [19] T. Mukherjee *et al.*, “Pt Us Pt Us,” 2016.
- [20] S. K. Rajeev, M. P. Rajasekaran, G. Vishnuvarthanan, and T. Arunprasath, “Biomedical Signal

- Processing and Control A biologically-inspired hybrid deep learning approach for brain tumor classification from magnetic resonance imaging using improved gabor wavelet transform and Elmann-BiLSTM network,” vol. 78, no. June, 2022.
- [21] R. Vankdothu, M. Abdul, and H. Fatima, “A Brain Tumor Identification and Classification Using Deep Learning based on CNN-LSTM Method,” vol. 101, no. March, 2022.
- [22] M. Aamir *et al.*, “Computers and Electrical Engineering A deep learning approach for brain tumor classification using MRI images U,” *Comput. Electr. Eng.*, vol. 101, p. 108105, 2022, doi: 10.1016/j.compeleceng.2022.108105.
- [23] H. Alsaif, R. Guesmi, B. M. Alshammari, T. Hamrouni, and T. Guesmi, “applied sciences A Novel Data Augmentation-Based Brain Tumor Detection Using Convolutional Neural Network,” 2022.
- [24] S. Islam *et al.*, “Accurate brain tumor detection using deep convolutional neural network,” vol. 20, pp. 4733–4745, 2022.
- [25] M. Thamarai and S. P. Dhivyaa, “Analysis of Brain Tumor Classification using Pre-Trained CNN models,” vol. 9, no. 2, pp. 20–26, 2022.
- [26] D. Filatov, “Brain Tumor Diagnosis and Classification via Pre-Trained Convolutional Neural Networks,” pp. 0–5, 2022.
- [27] Z. Rasheed *et al.*, “Automated Classification of Brain Tumors from Magnetic Resonance Imaging Using Deep Learning,” *Brain Sci.*, vol. 13, no. 4, 2023, doi: 10.3390/brainsci13040602.
- [28] S. Mohsen, A. M. Ali, E. S. M. El-Rabaie, A. Elkaseer, S. G. Scholz, and A. M. A. Hassan, “Brain Tumor Classification Using Hybrid Single Image Super-Resolution Technique With ResNext101\_32× 8d and VGG19 Pre-Trained Models,” *IEEE Access*, vol. 11, no. March, pp. 55582–55595, 2023, doi: 10.1109/ACCESS.2023.3281529.
- [29] R. Appiah *et al.*, “Computer Methods and Programs in Biomedicine Brain tumor detection using proper orthogonal decomposition integrated with deep learning networks,” *Comput. Methods Programs Biomed.*, vol. 250, no. December 2023, p. 108167, 2024, doi: 10.1016/j.cmpb.2024.108167.
- [30] S. Prakash, A. Nandal, A. Dhaka, A. Alhudhaif, and K. Polat, “Brain tumor detection with multi-scale fractal feature network and fractal residual learning,” *Appl. Soft Comput.*, vol. 153, no. December 2023, p. 111284, 2024, doi: 10.1016/j.asoc.2024.111284.
- [31] R. Gayathiri and S. Santhanam, “Biomedical Signal Processing and Control C-SAN: Convolutional stacked autoencoder network for brain tumor detection using MRI,” vol. 99, no. December 2023, 2025.